Mat. Res. Soc. Symp. Proc. Vol. 692 © 2002 Materials Research Society

Optical Vibrational and Structural Properties of $Ge_{1-x}Sn_x$ alloys by UHV-CVD

Jennifer Taraci[1], S. Zollner[4], M. R. McCartney[2], Jose Menendez[3], D. J. Smith[2,3], John Tolle[1], M. Bauer[1], Erika Duda[4], N. V. Edwards[4], and J. Kouvetakis[1]
[1] Department of Chemistry, Arizona State University, Tempe AZ 85287
[2] Center for Solid State Science, Arizona State University, Tempe AZ 85287
[3] Department of Physics and Astronomy, Arizona State University, Tempe AZ 85287
[4] Motorola Inc, Semiconductor Products Sector, 2200 W. Broadway Rd, Mesa AZ 85502

ABSTRACT

UHV-CVD growth based on a deuterium stabilized Sn hydride and digermane produces Ge-Sn alloys with tunable bandgaps. The $Ge_{1-x}Sn_x$ (x=2-20 at.%) alloys are deposited on Si (100) and exhibit superior crystallinity and thermal stability compared with MBE grown films. Composition, crystal and electronic structure, and optical and vibrational properties are characterized by RBS, low energy SIMS, high resolution electron microscopy TEM, x-ray diffraction, as well as Raman and IR spectroscopies. TEM studies reveal epitaxial films with lattice constants between those of Ge and Sn. X-ray diffraction shows well-defined (004) peaks and rocking curves indicate a tightly aligned spread of the crystal mosaics. Resonance Raman indicate a E_1 bandgap reduction relative to Ge, consistent with a decrease of the E_2 critical point observed in spectroscopic ellipsometry. IR transmission spectra indicate an increase in absorption with increasing Sn content consistent with a decrease of the direct bandgap.

INTRODUCTION

The preparation of Ge-Sn alloys with cubic structures has attracted considerable attention because of reports that $Ge_{1-x}Sn_x$ heterostructures might exhibit tunable direct bandgaps [1,2]. $Ge_{1-x}Sn_x$ materials with Sn content greater than 1 at % are, however, thermodynamically unstable. This is due to the large difference in lattice constant of α-Sn (6.489 Å) and Ge (5.646 Å) and the instability of the cubic Sn above 13.2°C with respect to the β-Sn structure [3,4]. Despite this metastability considerable progress has been made in growing high quality $Ge_{1-x}Sn_x$ alloys by solid-source MBE and related physical methods [5-9]. Nevertheless major synthetic challenges still remain including segregation of Sn toward the film surface during MBE growth and low thermal stability of MBE-grown samples [9,10]. In some cases, annealing at temperatures as low as 120-300°C causes Sn precipitation and phase segregation. Recently we reported the first chemical method to prepare Ge-Sn materials utilizing precursors that incorporate single Sn atoms in the molecular structure and UHV-CVD [11,12]. Our method has afforded epitaxial, monocrystalline layers on Si (100) which display thermal stability substantially higher than that reported for MBE grown films of comparable compositions. In this report we summarize our growth results and describe in detail the optical, vibrational, and structural properties of the UHV-CVD grown materials.

RESULTS AND DISCUSSION

The depositions are conducted in a custom built UHV-CVD reactor at 350°C and 10^{-4} Torr. The substrates are Si (100) wafers prepared for deposition using a modified RCA process followed by H-passivation of the Si surface using 10% HF. The precursor is a deuterium-stabilized Sn hydride with molecular formula (Ph)SnD_3, Ph=C_6H_5. It has a vapor pressure of 3 Torr at 22°C and decomposes readily in UHV at 250°C to form Sn atoms via elimination of stable d_1-Ph and D_2 byproducts. The reaction of (Ph)SnD_3 with Ge_2H_6 produces epitaxial $Ge_{1-x}Sn_x$ films which incorporate Sn concentrations up to 20 at%. The films adhere extremely well to the Si surface and their visual appearance is similar to that of Ge. Thermal treatment indicated that the alloys are stable up to 650°C for samples with 5 % Sn concentrations, and at least up to 750°C for samples with less than 5 at. % Sn contents. Analyses at the nanometer scale by EDX in a high-resolution electron microscope show that there is no phase segregation or formation of Sn clusters during the annealing. All of the as deposited and annealed samples were analyzed by Rutherford backscattering (RBS) and selected samples were analyzed by secondary ion mass spectrometry (SIMS). RBS was used to determine the concentration of Sn and Ge and to detect and identify any possible D, H, or C impurities as well as to estimate the film thickness. The Sn to Ge elemental concentration was obtained by utilizing 2 MeV He^{2+} ions. Forward scattering and carbon resonance [$^{12}C(\alpha,\alpha)^{12}C$] experiments at 4.265 MeV confirmed the absence of D, H and C impurities. To determine the quality of the epitaxial growth, and to confirm substitutionality of Sn in the Ge lattice, the random and aligned (channeled) RBS spectra were recorded and compared. Figure 1 shows the two spectra for a sample containing 5 % Sn in which both Sn and Ge atoms channel remarkably well despite the large difference in lattice dimensions between the epilayer and the Si substrate. Low energy SIMS spectra were recorded on an Atomica 4500 spectrometer with a 300 eV O_2^+ primary ion beam. Figure 2 shows the SIMS profiles for $Ge_{0.95}Sn_{0.05}$ and $Ge_{0.88}Sn_{0.12}$

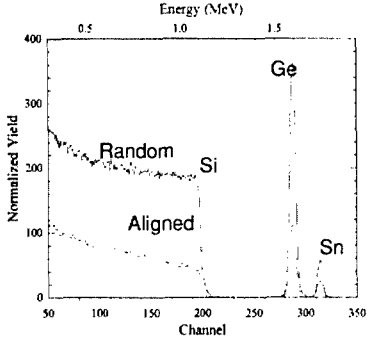

Figure 1. RBS aligned and random spectra for Ge0.95Sn0.05. Channeling is used to determine the crystallinity in the films.

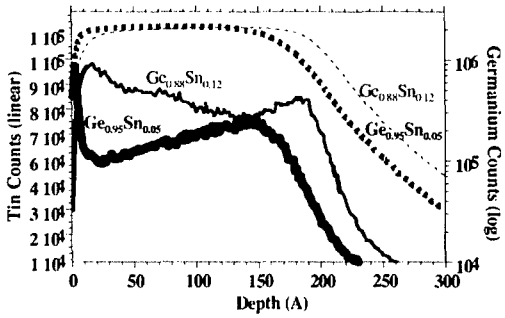

Figure 2. Low energy SIMS profiles of $Ge_{0.95}Sn_{0.05}$ and $Ge_{0.88}Sn_{0.12}$ showing nearly uniform Sn profile throughout the film. The slope is due to the film roughness which is about 10% of the film thickness.

The Ge and Sn profiles are constant in both samples. The slope seen in the Sn profile is due to film roughness. The SIMS spectra revealed background levels of H, and D as well as very low C and O levels primarily at the Si-film interface. The structure of the materials were determined by x-ray diffraction and high resolution TEM. X-ray analysis in the θ-2θ mode using a rotating anode show a single alloy peak corresponding to the (004) reflection of the diamond lattice. The lattice constants are intermediate between those of Ge and α-Sn. There are no extra peaks due to other phases except for the forbidden $Ge_{1-x}Sn_x$ (002) reflection with its intensity increasing with increasing Sn concentration in the samples. This reflection is due to the breaking of the inversion symmetry and it could be related to charge transfer from Sn to Ge. Also, this peak would be expected to appear if the symmetry is broken due to local distortions. This supports local ordering with the Sn atoms perhaps being arranged as second nearest neighbors in the crystal. Figure 3 shows representative patterns for a $Ge_{0.88}Sn_{0.12}$. Rocking scans of the (004) reflection have a FWHM less than 0.5° indicating a tightly aligned spread of crystal mosaics.

Cross-sectional TEM revealed that all samples were continuous films with an average roughness of about 10% of the film thickness. The films were monocrystalline and epitaxial. Periodic arrays of edge dislocations and occasional {111} stacking faults originating at the interface were observed but the remainder of the layer was defect-free. Some strain contrast was also observed in the TEM micrographs. A typical cross-sectional electron micrograph of the interface region demonstrating defect free coherent growth of $Ge_{0.94}Sn_{0.06}$ is shown in Figure 4. SAED patterns confirm that the material has a cubic structure. There is an appreciable splitting of the spots in the diffraction pattern which is consistent with the large difference in lattice dimensions between the substrate and the film. The lattice parameter obtained from measurements of the SAED patterns from this sample was 5.70 Å which is intermediate to those of pure Ge (5.646 Å) and α-Sn (6.489 Å). A similar value of 5.696 Å was measured by x-ray diffraction. EDX with a probe size less than 1 nm was used to determine whether the elemental composition was homogeneous on the nanometer scale and to further verify phase purity. A detailed survey of the compositional profiles in cross-section and plan-view geometries showed that the constituent elements were evenly distributed throughout the sample.

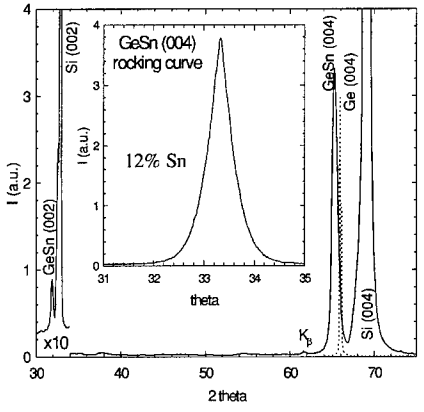

Figure 3. 2θ scan for $Ge_{0.88}Sn_{0.12}$ on Si (100). The inset shows the (004) rocking curve.

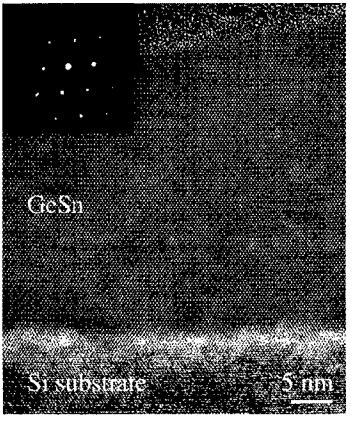

Figure 4. TEM micrograph of $Ge_{0.94}Sn_{0.06}$.

The optical properties and band structure of the $Ge_{1-x}Sn_x$ were investigated by spectroscopic ellipsometry and resonance Raman. The ellipsometric angles ψ and Δ were acquired for three samples containing 5, 12 and 16 at.% Sn. The data are displayed in the 1 to 6 eV photon-energy range as a pseudodielectric function and fitted in Figure 5 for $Ge_{0.95}Sn_{0.05}$. An examination of the imaginary part ε_2 shows that the absorption of GeSn rises from low values at 1 eV (just above the band gap of Ge and Si) to a broad peak (E_1) between 1.5 and 2.5 eV (which is actually a combination of an interference fringe and an interband transition) a shoulder E_0' at 3.5 eV and a knee at 4.2 eV called E_2. The presence of these three peaks indicates a well-pronounced band structure requiring a crystalline film with long-range ordering.

More information can be obtained by solving the Fresnel's equations assuming a substrate/film/overlayer sample structure and comparing simulated spectra with the experimental data. Since there is uncertainty for the optical constants below 1.5 eV and above 6 eV, only the data between 1 and 6 eV are shown. The model assumes that the epilayer is Ge (ignoring the effects of Sn alloying) and the surface overlayer is GeO_2. Using rough Ge as the overlayer leads to similar results. The dashed lines in Figure 5 show the results of the model. The film thickness for sample $Ge_{0.94}Sn_{0.06}$ obtained from the fit is 423 Å, with 62 Å of native oxide. The model shows the Ge E_1 and $E_1+\Delta_1$ critical points (doublet) at about 2.3 eV combined with an interference oscillation in ε_2 at 1.8 eV. In the experimental data, the splitting between the three structures is not resolved. The reduction in peak height of ε_2 at 4.2 eV is due to oxidation of the film combined with roughness. While a detailed analysis of the E_1 and $E_1+\Delta_1$ critical points is not possible in the alloy (since the spin-orbit splitting and the interference fringe are not resolved), the penetration depth of the light should be small enough at higher photon energies in the E_2 region near 4.2 eV. The second derivative of the pseudodielectric function was calculated (to remove the non-resonant background) and fitted with analytical lineshapes (Figure 6). This allows an accurate determination of the E_2 critical-point energy. From the value of E_2, the Sn content can be determined, since E_2 changes by a large amount between elemental Ge (4.368 eV) and elemental Sn (3.627 eV). We found that E_2 varies from 4.29 to 4.32 eV. The values of Sn concentration we obtain are 6.6, 8.1, and 11.1 % Sn. The corresponding RBS values are 5, 12, and 16 at. % respectively. The magnitude of shifts of E_2 found by ellipsometry are 50 to 80 meV. This method assumes a linear dependence of E_2 on Sn content. It is possible that the dependence of E_2 could be nonlinear for this unusual alloy system. Finally, the broadenings of E_2

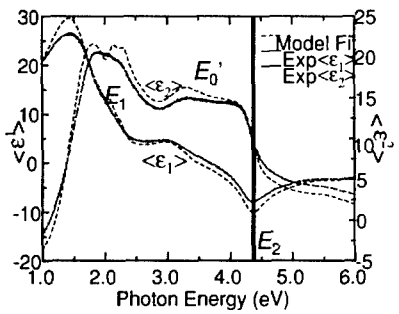

Figure 5. Experimental and model pseudodielectric functions of $Ge_{0.95}Sn_{0.05}$.

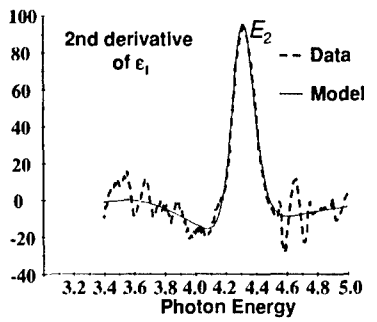

Figure 6. Second derivative of the pseudodielectric function with respect to photon energy. Fit to analytical lineshape.

Raman spectroscopy can be used to study the electronic structure of the alloys by measuring the intensity of the Raman peaks as a function of the laser wavelength. In pure Ge, it has been shown that the Raman cross section undergoes a resonant enhancement for laser photon energies near the E_1 and $E_1+\Delta_1$ gaps. We performed similar measurements for a $Ge_{0.95}Sn_{0.05}$ alloy and a Ge reference. The net result is that we find a redshift of E_1 and $E_1+\Delta_1$ by about 100 meV relative to pure Ge. This result combined with the redshift observed for the E_2 critical point by ellipsometry suggest that the bandgap in the alloy is reduced relative to pure Ge although it is not possible from this information to determine whether the expected indirect-direct transition has taken place. The Raman spectra of the Sn-Ge films showed a strong peak assigned to Ge-Ge lattice vibrations which is downshifted relative to the Raman peak of pure Ge. A weak peak around 240 cm^{-1} was also observed and was assigned to the Sn-Ge vibrations. The observation of Sn-Ge bands provides strong spectroscopic evidence for the presence of tetrahedral Ge-Sn coordination in our films and supports the formation of an extended random alloy with the diamond-cubic structure. Peaks corresponding to Sn-Sn vibrations were not detected in the Raman spectra. Finally we conducted transmission IR measurements in order to examine the effect of increasing Sn concentration on absorption. This should provide information of possible band gap variation with composition in the alloy. The transmission spectra of four Ge-Sn films with Sn content ranging from 9 to 18 % are shown in Figure 7. The spectrum of the Si substrate is also provided as a reference. We found that the transmission drops monotonically with increasing Sn content at about 0.8eV . The simplest explanation for these results is a decrease of the band gap of $Ge_{1-x}Sn_x$ as a function of Sn concentration, since such a reduction is likely to result in increased absorption at a fixed photon energy above the band gap. Further experiments and data analysis aimed toward determination of the absolute band gaps and absorption coefficients are in progress.

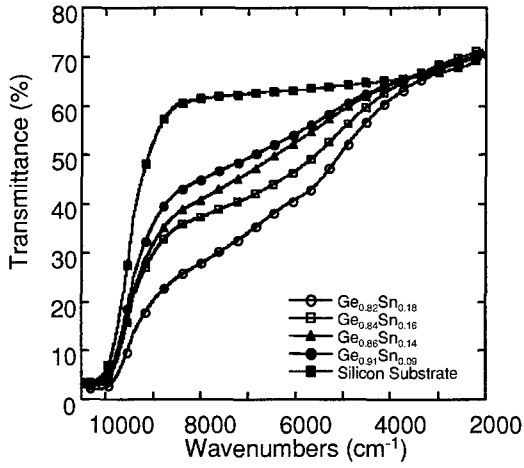

Figure 7. Transmission spectra of the Si substrate and four Ge-Sn films with Sn content ranging from 6-18%.

SUMMARY AND CONCLUSIONS

We describe UHV-CVD growth of $Ge_{1-x}Sn_x$ alloys from reactions of Ge_2H_3 with newly synthesized deuterium-stabilized Sn hydrides. Sn concentrations of 2-20 at % were measured by RBS in layers deposited on (100)Si substrates. Low energy SIMS indicated excellent uniformity of the constituent Ge and Sn elements and revealed background level contents of impurities such as H and D. High resolution TEM and XRD revealed high quality heteroepitaxial growth of films that are aligned well with the Si (001) direction. Strain relaxation by edge dislocations and some twining was also observed in the TEM studies. High-resolution analytical electron microscopy in cross section and plan-view confirmed that the materials are highly homogeneous and are of good thermal stability. Ellipsometry studies showed that the bandgap near the X-point (E2) redshifts 50 to 80 meV compared to Ge. IR spectra showed that the absorption trough the films at 0.8eV increases due to the red shift of the lowest bandgap. Raman spectra show Ge-Ge and Sn-Ge lattice vibrations and a red shift of the E1 resonance by 100 meV.

ACKNOWLEDGEMENTS

The work at ASU was supported by NSF and Army Research Office.

REFERENCES

1 G. He, H. A. Atwater, *Phys. Rev. Lett.* **79**, 1937 **(1997).**
2 R. Ragan, H. A. Atwater, *Appl. Phys. Lett.*, **77**, 3418 (2000).
3 *Bull. Alloy Phase Diagrams*, and references therein, **5**, 266 (1984).
4 O. Gurdal, R. Desjardins, J. R. A. Carlsson, N. Taylor, H. H. Radamson, J.-E. Sundgren, J. E. Greene, *J. Appl. Phys.* **83**, 162 (1998).
5 E. A. Fitzgerald, P. E. Freeland, M. T. Asom, W. P. Lowe, R. A. Macharri , B. E. Weir, A. R. Kortan, F. A. Thiel, T.-H. Xie, A. M. Sergent, S. L. Cooper, G. A. Thomas, L. C. Kimerling, *J. Elect. Mater.* **20**, 489 (1991).
6 M. T. Asom, E. A. Fitzgerald, A. R. Kortan, B. Spear, L. C. Kimerling, *Appl. Phys. Lett.* **55**, 578 (1989).
7 J. Piao, R. Beresfor, T. Licata, W. I. Wang, H. Homma, *J. Vac. Sci. Technol. B.* **8**, 221 (1990).
8 S. S. Wong, G. He, S. Nikzad, C. C. Ahn, H. A. Atwater, *J. Vac. Sci. Technol. A.* **13**, 216 (1995).
9 P. R. Pukite, A. Harwit, S. S. Iyer, *Appl. Phys. Lett.* **54**, 2142 (1989).
10 W. Wegscheider, J. Olajos, U. Menczigar, U. Dondl, G. Abstreiter, *J. Cryst Growth.* **132**, 75 (1992).
11 J. Taraci, J. Tolle, M. R. McCartney, J. Menendez, M. Santana, D. J. Smith, J. Kouvetakis, *Apl. Phys. Lett.* **78**, 3607 (2001).
12 J. Taraci, S. Zollner, M. R. McCartney, J. Menendez, M. A. Santana, D. J. Smith, G. Wolf, A. Haaland, A. Tutukin, G. Gundersen, J. Kouvetakis, *J. Am. Chem. Soc. 132*, 10980 (2001).